

# Oxidative Addition of Group 14 Hydrides to an Unsaturated Metal Cluster. Kinetics of Addition of $\text{HER}_3$ ( $\text{ER}_3 = \text{SiEt}_3, \text{SiPh}_3, \text{GeBu}_3, \text{SnBu}_3, \text{SnPh}_3$ ) to $\text{H}_2\text{Os}_3(\text{CO})_{10}$

Robert J. Hall, Petr Serguievski, and Jerome B. Keister\*

Department of Chemistry, University at Buffalo, The State University of New York at Buffalo, Buffalo, New York 14260-3000

Received May 15, 2000

The kinetics and mechanism of oxidative addition of  $\text{HER}_3 = \text{HSiEt}_3, \text{HGeBu}_3, \text{HSnBu}_3, \text{HSnPh}_3$  to the unsaturated cluster  $\text{H}_2\text{Os}_3(\text{CO})_{10}$ , initially forming  $\text{H}_3\text{Os}_3(\text{CO})_{10}(\text{ER}_3)$ , are reported. For  $\text{HSiEt}_3$  the addition is readily reversible, with an equilibrium constant of  $100 \text{ M}^{-1}$  at 303 K. In each case the rate law for the forward reaction is first-order in both reagents. Rate constants ( $\text{M}^{-1} \text{ s}^{-1}$ ) at 303 K are as follows:  $\text{HSnBu}_3$  (23) >  $\text{HSnPh}_3$  (1.5) >  $\text{HGeBu}_3$  (0.15) >  $\text{HSiEt}_3$  ( $3.8 \times 10^{-3}$ ). Comparisons are made to additions of group 14 element hydrides to 16-electron Ir(I) complexes. The reaction with  $\text{HSiPh}_3$ , which forms  $\text{H}_3\text{Os}_3(\text{CO})_9(\text{SiPh}_3)$  and further addition products, was also examined.

## Introduction

Of the numerous studies of reactions of metal clusters with small molecules, few have concerned the mechanisms of these reactions.<sup>1</sup> Ligand substitutions on metal clusters have been extensively studied, but the only other elementary reaction which has received attention is oxidative addition/reductive elimination of molecular hydrogen.<sup>2,3</sup> In general, the mechanism of oxidative addition of hydrogen is similar to that found for monometallic complexes, but there are important effects due to the polymetallic character. For example, cluster-bound hydrides most commonly bridge two metal atoms, and a bridging hydride is stabilized by ca. 40 kJ/mol, compared with terminal coordination, thus affecting the kinetics and thermodynamics of hydride elimination reactions.<sup>3d,4</sup> Another example of a "special" property of cluster-based chemical reactivity is the greater prevalence of agostic  $\text{M}-\text{H}-\text{C}$  species on clusters.<sup>5</sup> Finally, intramolecular, intermetallic ligand migrations are involved in many cluster reactions.<sup>6</sup> Because of these unique characteristics, metal clusters are frequently used as models for the bonding of small molecules to

metal surfaces and perhaps should also be considered as superior models for reaction mechanisms on surfaces.<sup>7</sup>

One prototypical cluster is  $\text{H}_2\text{Os}_3(\text{CO})_{10}$ , a rare example of a stable, unsaturated cluster. Originally reported by Lewis, Johnson, and co-workers,<sup>8</sup> the crucial, improved synthesis by Kaesz and co-workers<sup>9</sup> allowed it to become a mainstay in cluster chemistry. One of us (J.B.K.) conducted one of the first studies of the reactions of this compound, some 20 years ago as his doctoral research under John Shapley, and it is fitting that our final paper concerning mechanisms of oxidative addition/reductive elimination reactions of clusters returns again to this important molecule. Pomeroy and co-workers previously studied the reactions of the unsaturated cluster  $\text{H}_2\text{Os}_3(\text{CO})_{10}$  with  $\text{HSiPh}_3, \text{H}_2\text{SiPh}_2, \text{H}_3\text{SiPh}, \text{HSiCl}_3, \text{HSiMeCl}_2, \text{HSiMe}_3, \text{HGePh}_3, \text{HSnPh}_3, \text{HSnMe}_3$ , and  $\text{HSnBu}_3$ .<sup>10–12,24</sup> For

(1) (a) Shriver, D. F.; Kaesz, H. D.; Adams, R. D. *The Chemistry of Metal Clusters*; VCH: New York, 1990. (b) Adams, R. D.; Cotton, F. A. *Catalysis by Di- and Polynuclear Metal Cluster Complexes*; Wiley-VCH: New York, 1998.

(2) (a) Poë, A. J.; Sampson, C. N.; Smith, R. T.; Zheng, Y. *J. Am. Chem. Soc.* **1993**, *115*, 3174. (b) Hudson, R. H. E.; Poë, A. J.; Sampson, C. N.; Siegel, A. *J. Chem. Soc., Dalton Trans.* **1989**, 2235.

(3) (a) Bavaro, L. M.; Montanero, P.; Keister, J. B. *J. Am. Chem. Soc.* **1983**, *105*, 4977. (b) Anhaus, J.; Bajaj, H. C.; van Eldik, R.; Nevinger, L. R.; Keister, J. B. *Organometallics* **1989**, *8*, 2903. (c) Bavaro, L. M.; Keister, J. B. *J. Organomet. Chem.* **1985**, *287*, 357. (d) Keister, J. B.; Onyeso, C. C. O. *Organometallics* **1988**, *7*, 2364. (e) Nevinger, L. R.; Keister, J. B.; Maher, J. *Organometallics* **1990**, *9*, 1900. (f) Safarowic, F. J.; Biedeman, D. J.; Keister, J. B. *J. Am. Chem. Soc.* **1996**, *118*, 11805. (g) Doi, Y.; Koshizuka, K.; Keil, T. *Inorg. Chem.* **1982**, *21*, 2732. (h) Taube, D. J.; Rokicki, A.; Anstock, M.; Ford, P. C. *Inorg. Chem.* **1987**, *26*, 526. (i) Casey, C. P.; Hallenbeck, S. L.; Widenhoefer, R. A. *J. Am. Chem. Soc.* **1995**, *117*, 4607.

(4) Vites, J.; Fehlner, T. P. *Organometallics* **1984**, *3*, 491.

(5) Fehlner, T. P. *Polyhedron* **1990**, *9*, 1955.

(6) Band, E.; Muetterties, E. L. *Chem. Rev.* **1978**, *78*, 639.

(7) Muetterties, E. L.; Rhodin, T. N.; Band, E.; Brucker, C. F.; Pretzer, W. R. *Chem. Rev.* **1979**, *79*, 91.

(8) Johnson, B. F. G.; Lewis, J.; Kilty, P. *J. Chem. Soc. A* **1968**, 2859.

(9) Knox, S. A. R.; Koepke, J. W.; Andrews, M. A.; Kaesz, H. D. *J. Am. Chem. Soc.* **1975**, *97*, 3942.

(10) Ramadan, R. M.; Pomeroy, R. K. Unpublished results.

(11) Willis, A. C.; Einstein, F. W. B.; Ramadan, R. M.; Pomeroy, R. K. *Organometallics* **1983**, *2*, 935.

(12) van Buuren, G. N.; Willis, A. C.; Einstein, F. W. B.; Peterson, L. K.; Pomeroy, R. K.; Sutton, D. *Inorg. Chem.* **1981**, *20*, 4361.

(13) (a) Collman, J. P.; Hegedus, L. S.; Norton, J. R.; Finke, R. G. *Principles and Applications of Organotransition Metal Chemistry*; University Science Books: Mill Valley, CA, 1987; Chapter 5. (b) James, B. R. In *Comprehensive Organometallic Chemistry*; Wilkinson, G., Stone, F. G. A., Abel, E., Eds.; Pergamon: Oxford, U.K., 1982; Vol. 8, Chapter 51.

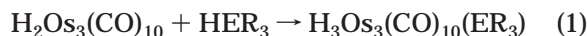
(14) (a) Mackay, K. M.; Nicholson, B. K. In *Comprehensive Organometallic Chemistry*; Wilkinson, G., Stone, F. G. A., Abel, E., Eds.; Pergamon: Oxford, U.K., 1982; Vol. 6, Chapter 43. (b) Stahl, S. S.; Labinger, J. A.; Bercaw, J. E. *J. Am. Chem. Soc.* **1996**, *118*, 5961 and references therein.

(15) (a) Fawcett, J. P.; Harrod, J. F. *Can. J. Chem.* **1997**, *54*, 3102.

(b) Harrod, J. F.; Smith, C. A.; Than, K. A. *J. Am. Chem. Soc.* **1972**, *94*, 8321.

(16) (a) Cabeza, J. A.; Llamazares, A.; Riera, V.; Triki, S.; Ouahab, L. *Organometallics* **1992**, *11*, 3334. (b) Cabeza, J. A.; Franco, R. J.; Riera, V.; Garcia-Granda, S.; Van der Maelen, J. F. *Organometallics* **1995**, *14*, 3342.

most of these the isolated product is the oxidative addition product  $\text{H}_3\text{Os}_3(\text{CO})_{10}(\text{ER}_3)$  (eq 1). We report here a study of the kinetics and mechanism of this reaction.



### Experimental Section

**Chemicals.**  $\text{H}_2\text{Os}_3(\text{CO})_{10}$  was prepared as described in the literature.<sup>9</sup> Triphenyl- and triethylsilane, triphenyl- and tributylstannane, tributyltin deuteride, and tributylgermane were purchased from Aldrich and used as received. Heptane and octane were obtained from Fisher. Purification by distillation from  $\text{CaH}_2$  under nitrogen had no effect on the kinetics; therefore, solvents were used as received.

**General Considerations.** The IR spectra were obtained on a Nicolet 550 Magna FT-IR spectrometer. The  $^1\text{H}$  NMR spectra were obtained on a Varian 400 MHz spectrometer.

**Characterization of Products from  $\text{HSiEt}_3$ .** To obtain a sample of  $\text{H}_3\text{Os}_3(\text{CO})_{10}(\text{SiEt}_3)$ ,  $\text{H}_2\text{Os}_3(\text{CO})_{10}$  was dissolved in neat triethylsilane. After the solution turned yellow, the triethylsilane was removed by vacuum transfer. The yellow residue was then used for spectroscopic characterization. IR (heptane): 2126 w, 2100 w, 2094 w, 2079 w, 2074 m, 2043 vs, 2038 sh, 2025 s, 2008 w, 1990 w, 1975 vw, 1965 vw  $\text{cm}^{-1}$ . The  $^1\text{H}$  NMR spectrum of the product mixture was obtained as follows. A solution of 17.1 mg of  $\text{H}_2\text{Os}_3(\text{CO})_{10}$  and 11.5 mg of  $\text{HSiEt}_3$  in 0.64 mL of dichloromethane- $d_2$  was allowed to stand at room temperature for 1.5 h. Then the spectra were recorded at temperature intervals down to  $-70^\circ\text{C}$ . In the hydride region at this temperature 88% of the total integrated resonances could be assigned to the following:  $\text{H}_3\text{Os}_3(\text{CO})_{10}(\text{SiEt}_3)$  (79%, three isomers),  $\text{H}_2\text{Os}_3(\text{CO})_{10}$  (4.5%), and  $\text{H}_3\text{Os}_3(\text{CO})_9(\text{SiEt}_3)$  (4.5%). In addition, a number of very small resonances were observed, perhaps due to other isomers of the addition product. At this time no signals due to  $\text{H}_2\text{Os}_3(\text{CO})_{10}(\text{SiEt}_3)_2$  or  $\text{H}_3\text{Os}_3(\text{CO})_9(\text{SiEt}_3)_3$  were present; after 2 days the room-temperature spectrum contained resonances assignable to  $\text{H}_2\text{Os}_3(\text{CO})_{10}(\text{SiEt}_3)_2$  ( $-16.830$  (d),  $-17.568$  (d) ppm,  $J = 1.6$  Hz) and  $\text{H}_3\text{Os}_3(\text{CO})_9(\text{SiEt}_3)_3$  ( $-16.185$  ppm), in addition to signals from  $\text{H}_3\text{Os}_3(\text{CO})_{10}(\text{SiEt}_3)$ ,  $\text{H}_2\text{Os}_3(\text{CO})_{10}$ , and  $\text{H}_3\text{Os}_3(\text{CO})_9(\text{SiEt}_3)$  and other, new unassigned peaks.

The residues from kinetic runs were combined and separated by thin-layer chromatography on silica gel, with hexanes as eluent. Four bands were eluted, colored yellow, purple

( $\text{H}_2\text{Os}_3(\text{CO})_{10}$ ), yellow, and yellow, in order of decreasing  $R_f$ . Extraction of the plate above the top yellow band yielded colorless  $\text{H}_3\text{Os}_3(\text{CO})_9(\text{SiEt}_3)_3$  (IR (hexanes) 2078 w, 2032 vs, 2026 vw sh, 2008 m  $\text{cm}^{-1}$ ;  $^1\text{H}$  NMR ( $\text{CDCl}_3$ ,  $20^\circ\text{C}$ ) 1.179 (t, 27 H,  $J = 7$  Hz), 1.070 (q, 18 H),  $-16.31$  (s, 3 H) ppm).

**Reaction of 1 Equiv of  $\text{HGeBu}_3$  with  $\text{H}_2\text{Os}_3(\text{CO})_{10}$ .** In an NMR tube was placed 10.5 mg (0.0123 mmol) of  $\text{H}_2\text{Os}_3(\text{CO})_{10}$  and 3.6 mg (0.0147 mmol) of  $\text{HGeBu}_3$  in approximately 1 mL of deuteriochloroform.  $^1\text{H}$  NMR ( $20^\circ\text{C}$ ):  $-9.2$  (br, 1H),  $-9.5$  (br, 1H),  $-11.5$  (s, 3H),  $-15.5$  (br, 1H),  $-16.8$  (s, 1H),  $-18.3$  (s, 1H),  $-18.4$  (s, 1H) ppm.  $^1\text{H}$  NMR ( $-70^\circ\text{C}$ ):  $\text{H}_3\text{Os}_3(\text{CO})_{10}(\text{GeBu}_3)$  (92% of total hydride integral); isomer **1t** (17%),  $-9.52$  (d, 1H,  $J_{\text{HH}} = 12$  Hz),  $-17.06$  (d, 1H,  $J_{\text{HH}} = 12$  Hz),  $-18.35$  (s, 1H) ppm; isomer **2t** (6.1%),  $-9.51$  (d, 1H,  $J_{\text{HH}} = 13$  Hz),  $-17.38$  (d, 1H,  $J_{\text{HH}} = 13$  Hz),  $-17.76$  (s, 1H) ppm; isomer **1c** (75%),  $-10.04$  (d, 1H,  $J_{\text{HH}} = 3$  Hz),  $-17.03$  (s, 1H),  $-19.49$  (d, 1H) ppm. IR (heptane): 2124 w, 2100 vw, 2092 w, 2073 m, 2064 vw, 2043 vs, 2024 s, 2010 m, 2006 m, 1990 w  $\text{cm}^{-1}$ .

**Kinetics of  $\text{HSiR}_3$  Addition to  $\text{H}_2\text{Os}_3(\text{CO})_{10}$ .** In a 25 mL Erlenmeyer flask was weighed out  $\text{H}_2\text{Os}_3(\text{CO})_{10}$  (ca. 8 mg) and heptane (ca. 5 mL) to give a known concentration of ca. 1.5 mM. The solution was placed in a 50 mL Schlenk flask under a nitrogen atmosphere, and the flask was immersed in a Haake temperature bath ( $\pm 0.1^\circ\text{C}$ ) and allowed to come to thermal equilibrium. A weighed amount of silane (10–40-fold excess) was then mixed with the solution, and aliquots were taken at intervals. The kinetics for the disappearance of  $\text{H}_2\text{Os}_3(\text{CO})_{10}$  was followed periodically for over 3 half-lives using the 2062  $\text{cm}^{-1}$  absorption ( $R = \text{Et}$ ) or the 2074  $\text{cm}^{-1}$  absorption ( $R = \text{Ph}$ ) in the IR spectrum.

**Kinetics of  $\text{HGeBu}_3$  Addition to  $\text{H}_2\text{Os}_3(\text{CO})_{10}$ .** To 2 mL of distilled heptane was added 6.0 mg (0.0070 mmol) of  $\text{H}_2\text{Os}_3(\text{CO})_{10}$ . The cluster was dissolved at room temperature, and the solution was then placed in a vial in the circulating bath for 10 min. Another vial containing the pure excess of  $\text{HGeBu}_3$  was also allowed to come to temperature in the circulating bath for 10 min. At this point, both solutions were quickly mixed and placed in a thermostated cuvette. The cuvette was then flushed with argon gas, and the kinetics of addition of  $\text{HGeBu}_3$  was followed by monitoring the absorbance at 560 nm for  $\text{H}_2\text{Os}_3(\text{CO})_{10}$ .

**Kinetics for Addition of  $\text{HSnR}_3$  to  $\text{H}_2\text{Os}_3(\text{CO})_{10}$ .** A 4.9 mM solution of  $\text{H}_2\text{Os}_3(\text{CO})_{10}$  was placed in one syringe and a solution of  $\text{HSnR}_3$  in the other syringe of an Applied Photo-physics SX-18MV stopped-flow kinetics instrument. For each concentration of tin hydride, 10 injections were done. The temperature of the kinetic runs was maintained by a Haake temperature bath. The reactions were followed for 3 half-lives.

**Treatment of Data.** For triethylsilane the corrected absorbance at 2062  $\text{cm}^{-1}$  was fit to eq 2 by a nonlinear least-squares procedure, using Psi-Plot for Windows, Version 4.01 (Poly Software International);  $A_t$  is the absorbance at time  $t$ ,  $A_{\text{eq}}$  is the absorbance at equilibrium, and  $k_{\text{obs}}$  is the rate constant for relaxation to equilibrium. The values of the

$$A_t = (A_t - A_{\text{eq}}) \exp(-k_{\text{obs}}t) + A_{\text{eq}} \quad (2)$$

$$k_{\text{obs}} = k_1[\text{HSiEt}_3] + k_2 \quad (3)$$

$$K_{\text{eq}} = k_1/k_2 \quad (4)$$

adjustable parameters  $A_{\text{eq}}$  and  $k_{\text{obs}}$  thus determined by the best fit, combined with the initial absorbance before mixing, were used to determine  $K_{\text{eq}}$ ,  $k_1$ , and  $k_2$ . The values from a range of concentrations were averaged, with the error expressed as the standard deviation.

For all other reactions plots of  $\ln(\text{absorbance})$  vs time were analyzed by least-squares fit.

### Results

**Addition of  $\text{HER}_3$  to  $\text{H}_2\text{Os}_3(\text{CO})_{10}$  ( $E = \text{Si, Ge, Sn}$ ;  $R = \text{Alkyl, Phenyl}$ ).** Pomeroy and co-workers previ-

(17) (a) Suss-Fink, G.; Ott, J.; Schmidkonz, B.; Guldner, K. *Chem. Ber.* **1982**, *115*, 2487. (b) Suss-Fink, G. *Angew. Chem., Int. Ed. Engl.* **1982**, *21*, 73. (c) Suss-Fink, G.; Reiner, J. *J. Organomet. Chem.* **1981**, *221*, C36.

(18) (a) Duggan, T. P.; Golden, M. J.; Keister, J. B. *Organometallics* **1990**, *9*, 1656. (b) Churchill, M. R.; Janik, T. S.; Duggan, T. P. *Organometallics* **1987**, *6*, 799. (c) Churchill, M. R.; Ziller, J. W.; Dalton, D. M.; Keister, J. B. *Organometallics* **1987**, *6*, 806. (d) Ziller, J. W.; Bower, D. K.; Dalton, D. M.; Keister, J. B.; Churchill, M. R. *Organometallics* **1989**, *8*, 492. (e) Strickland, D. A.; Shapley, J. R. *J. Organomet. Chem.* **1991**, *401*, 187. (f) Bower, D. K.; Keister, J. B. *Organometallics* **1990**, *9*, 2321. (g) Safarowic, F. J.; Keister, J. B. *Organometallics* **1996**, *15*, 3310.

(19) (a) Calvert, R. B.; Shapley, J. R. *J. Am. Chem. Soc.* **1978**, *100*, 6544. **1977**, *99*, 5225. (b) Koike, M.; VanderVelde, D. G.; Shapley, J. R. *Organometallics* **1994**, *13*, 1404. (c) Cree-Uchiyama, M.; Shapley, J. R.; St. George, G. M. *J. Am. Chem. Soc.* **1986**, *108*, 1316.

(20) (a) Hudson, R. H. E.; Poe, A. J. *Organometallics* **1995**, *14*, 3238. (b) Neubrand, A.; Poe, A. J.; van Eldik, R. *Organometallics* **1995**, *14*, 3249.

(21) (a) Keister, J. B.; Shapley, J. R. *Inorg. Chem.* **1982**, *21*, 3304. (b) Churchill, M. R.; DeBoer, B. G. *Inorg. Chem.* **1977**, *16*, 2397. (c) Churchill, M. R.; DeBoer, B. G. *Inorg. Chem.* **1977**, *16*, 878. (d) Adams, R. D.; Golembeski, N. M. *Inorg. Chem.* **1979**, *18*, 1909. (e) Deeming, A. J.; Hasso, S. *J. Organomet. Chem.* **1976**, *114*, 313.

(22) Aime, S.; Gobetto, R.; Valls, E. *Inorg. Chim. Acta* **1998**, *275–276*, 521.

(23) Hudson, R. H. E.; Poë, A. J. *Inorg. Chim. Acta* **1997**, *259*, 257.

(24) Einstein, F. W. B.; Pomeroy, R. K.; Willis, A. C. *J. Organomet. Chem.* **1986**, *311*, 257.

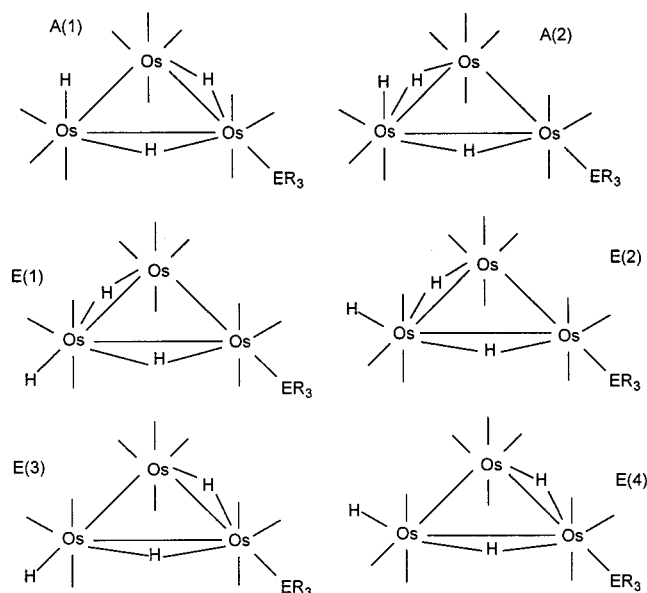


**Figure 1.** Structures of isomers  $\text{H}_3\text{Os}_3(\text{CO})_{10}(\text{ER}_3)$ , as proposed by Pomeroy et al.

ously studied the reactions of  $\text{H}_2\text{Os}_3(\text{CO})_{10}$  with  $\text{HSiPh}_3$ ,  $\text{H}_2\text{SiPh}_2$ ,  $\text{H}_3\text{SiPh}$ ,  $\text{HSiCl}_3$ ,  $\text{HSiMeCl}_2$ ,  $\text{HSiMe}_3$ ,  $\text{HGePh}_3$ ,  $\text{HSnPh}_3$ ,  $\text{HSnMe}_3$ , and  $\text{HSnBu}_3$ .<sup>10–12,24</sup> For most of these the isolated product is the oxidative addition product  $\text{H}_3\text{Os}_3(\text{CO})_{10}(\text{ER}_3)$ . These compounds exist as mixtures of isomers (Figure 1) which differ in the orientations of the hydride ligands and which are interconverting at a rate on the NMR time scale at room temperature. Crystallographic characterization of  $\text{H}_3\text{Os}_3(\text{CO})_{10}(\text{SiHPh}_2)$ , which appears to exist as a single isomer in solution, determined the structure denoted E(1) in Figure 1.<sup>24</sup> The kinetic product of the reaction with  $\text{HSnMe}_3$  has been identified by Pomeroy et al. as isomer A(1). The characterizations and fluxional behavior of these compounds will be the subject of a separate paper by these workers. The products of reactions with  $\text{HGeBu}_3$  and  $\text{HSiEt}_3$  reported herein are analogous to the others, although these compounds could not be isolated in analytically pure forms.

**Triethylsilane.** Pomeroy et al. previously examined reactions with  $\text{SiH}_2\text{Ph}_2$  and  $\text{SiH}_3\text{Ph}$  which form  $\text{H}_3\text{Os}_3(\text{CO})_{10}(\text{SiR}_3)$  and then sequentially  $\text{H}_2\text{Os}_3(\text{CO})_{10}(\text{SiR}_3)_2$  and  $\text{H}_3\text{Os}_3(\text{CO})_9(\text{SiR}_3)_3$ .<sup>10,24</sup> In neat triethylsilane  $\text{H}_2\text{Os}_3(\text{CO})_{10}$  reacts within minutes; vacuum removal of the silane allows isolation of the product for purposes of spectroscopic characterization. The IR spectrum (Supporting Information, Figure 1S(a)) is very similar to those of other products  $\text{H}_3\text{Os}_3(\text{CO})_{10}(\text{ER}_3)$  (Supporting Information, Figure 2S). The low-temperature  $^1\text{H}$  NMR spectra were obtained for a product mixture from reaction of  $\text{HSiEt}_3$  ( $1.55 \times 10^{-1}$  M) and  $\text{H}_2\text{Os}_3(\text{CO})_{10}$  ( $3.1 \times 10^{-2}$  M) in dichloromethane- $d_2$  after 1.5 h at room temperature. At  $-70^\circ\text{C}$  the spectrum displays signals due to  $\text{H}_2\text{Os}_3(\text{CO})_{10}$  (ca. 7%) and at least three isomers  $\text{H}_3\text{Os}_3(\text{CO})_{10}(\text{SiEt}_3)$  (ca. 76%), the structures of which are as proposed by Pomeroy et al. in Figure 1, with a small amount of what appears to be  $\text{H}_3\text{Os}_3(\text{CO})_9(\text{SiEt}_3)$  and a number of small hydride resonances which have not been assigned. The major isomer of  $\text{H}_3\text{Os}_3(\text{CO})_{10}(\text{SiEt}_3)$  ( $-10.047$  (d,  $J = 4$  Hz),  $-16.804$  (d,  $J = 2$  Hz), and  $-19.409$  (dd,  $J = 4, 2$  Hz) ppm (ca. 42%)) is one of those in Figure 1 which contains a terminal hydride in

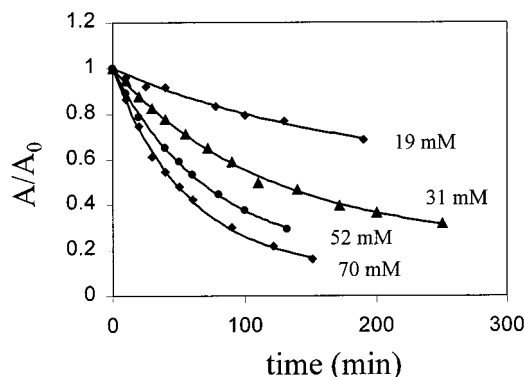


**Figure 2.** Plot of absorbance vs time for various  $\text{HSiEt}_3$  concentrations at  $40^\circ\text{C}$ .

an axial site, most likely A(1). At least two other isomers of  $\text{H}_3\text{Os}_3(\text{CO})_{10}(\text{SiEt}_3)$  are present which each contain an equatorial, terminal hydride that is trans to a bridging hydride ( $-9.517$  (d,  $J = 13$  Hz),  $-16.950$  (d,  $J = 13$  Hz), and  $-18.275$  (s) ppm (ca. 29%);  $-9.439$  (d,  $J = 12$  Hz),  $-17.272$  (d,  $J = 12$  Hz), and  $-17.724$  (s) ppm (ca. 5%)). In addition, the spectrum contains signals assigned to  $\text{H}_3\text{Os}_3(\text{CO})_9(\text{SiEt}_3)$  at  $-8.249$  (s),  $-12.721$  (s), and  $-13.081$  (s) ppm (ca. 4%). At  $-50^\circ\text{C}$  the coupled hydrides of the major, cis isomer begin to broaden due to exchange, analogous to that shown for structurally analogous  $\text{H}(\mu\text{-H})\text{Os}_3(\text{CO})_{10}(\text{PR}_3)$ ;<sup>21</sup> at this temperature the hydrides due to the other two isomers remain sharp, as does the singlet hydride resonance for the cis isomer. At  $-50^\circ\text{C}$  the resonance at  $-16.804$  ppm begins to broaden as well. At  $0^\circ\text{C}$  the remaining hydrides due to the trans isomers begin to broaden. At room temperature broad signals are observed at  $-9.36$ ,  $-16.87$  (br d), and  $-18.17$  ppm, in addition to those assigned to  $\text{H}_2\text{Os}_3(\text{CO})_{10}$  and some minor unassigned peaks. The spectra are analogous to those found by Pomeroy and co-workers for the related  $\text{H}_3\text{Os}_3(\text{CO})_{10}(\text{ER}_3)$ . Full characterization of the dynamic behavior of these systems will be reported by that group in a later paper.

This  $\text{HSiEt}_3$  addition is readily reversible. In the absence of excess  $\text{HSiEt}_3$ , elimination occurs, regenerating  $\text{H}_2\text{Os}_3(\text{CO})_{10}$ , so that the product cannot be purified by chromatography. In addition,  $\text{H}_3\text{Os}_3(\text{CO})_{10}(\text{SiEt}_3)$  slowly reacts further with  $\text{HSiEt}_3$ , forming sequentially  $\text{H}_2\text{Os}_3(\text{CO})_{10}(\text{SiEt}_3)_2$  and then  $\text{H}_3\text{Os}_3(\text{CO})_9(\text{SiEt}_3)_3$ . Because of these complications we were unable to obtain analytically pure material.

The kinetics of the addition were determined under pseudo-first-order conditions. The IR spectra (Supporting Information, Figure 1S(a)) show establishment of the equilibrium, followed by slower reactions which form sequentially  $\text{H}_2\text{Os}_3(\text{CO})_{10}(\text{SiEt}_3)_2$  and then  $\text{H}_3\text{Os}_3(\text{CO})_9(\text{SiEt}_3)_3$ . The identity of the initial product (growth of absorbance at  $2043\text{ cm}^{-1}$ ) is confirmed by spectral subtraction (Supporting Information, Figure 1(b)). Ultimately only  $\text{H}_3\text{Os}_3(\text{CO})_9(\text{SiEt}_3)_3$  is present (Supporting Information, Figure 1S(a,c)). The kinetics were determined by monitoring the  $2062\text{ cm}^{-1}$  absorption of  $\text{H}_2\text{Os}_3(\text{CO})_{10}$ . Plots of absorbance vs time showed gradual relaxation to equilibrium and slower loss of intensity due to further reactions. Normalized plots at different  $\text{HSiEt}_3$  concentrations are shown in Figure 2. The data were fit to eq 2 for greater than 3 half-lives (defined as  $0.693/k_{\text{obs}}$ ), over which time the contributions of follow-



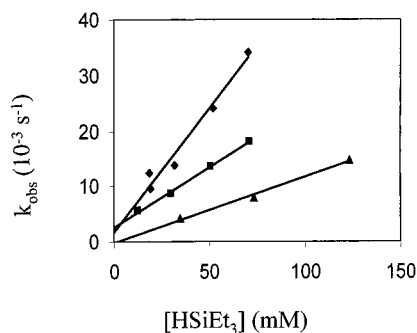


**Figure 3.** Plot of  $k_{\text{obs}}$  vs  $[\text{HSiEt}_3]$  at 20.0, 30.0, and 40.0 °C.

up reactions are relatively insignificant. The calculated value of the absorbance at equilibrium,  $A_{\text{eq}}$ , is not very precisely established at high  $[\text{HSiEt}_3]$  due to the relatively low value of  $A_{\text{eq}}$ , and at low  $[\text{HSiEt}_3]$  due to subsequent reactions. Even so, reproducible and relatively precise values of  $k_{\text{obs}}$  were obtained. Plots of  $k_{\text{obs}}$  vs  $[\text{HSiEt}_3]$  (Figure 3) were linear with slope  $k_1$ . At 20.0 °C the intercept is indistinguishable from zero, within the error limits of the plot, but the better behaved data obtained at 30.4 and 40.5 °C gave intercepts of  $k_2$  which were in reasonably good agreement with values calculated from the equilibrium constant ( $K_{\text{eq}} = k_1/k_2$ , 103(15)  $\text{M}^{-1}$  at 30.4 °C, 82(15)  $\text{M}^{-1}$  at 40.5 °C) determined from initial and extrapolated equilibrium concentrations of  $\text{H}_2\text{Os}_3(\text{CO})_{10}$ . At 30.4 °C  $k_1$  from Figure 3 is  $[3.67(0.15)] \times 10^{-3} \text{ M}^{-1} \text{ s}^{-1}$  and  $k_2$  is  $[4.1(0.7)] \times 10^{-5} \text{ s}^{-1}$ , compared with values of  $[3.75(0.03)] \times 10^{-3} \text{ M}^{-1} \text{ s}^{-1}$  and  $[3.69(0.06)] \times 10^{-5} \text{ s}^{-1}$ , respectively, calculated from  $A_{\text{eq}}$  and  $k_{\text{obs}}$ . At 50.0 °C only lower concentrations (slower reactions) could be followed and estimates of the equilibrium constant could not be determined. As expected, the equilibrium constant decreases with increasing temperature, but the poor precision of the data at 20.0 and 50.0 °C does not allow for reliable determinations of  $\Delta H^\ddagger$  and  $\Delta S^\ddagger$ . An Eyring plot gives values of  $\Delta H_1^\ddagger = 44.9(2.5) \text{ kJ/mol}$  and  $\Delta S_1^\ddagger = -144(8) \text{ J/(K mol)}$ .

**Triphenylsilane.** The reaction of  $\text{HSiPh}_3$  (1:1) with  $\text{H}_2\text{Os}_3(\text{CO})_{10}$  at 70 °C for 7 h has been reported to yield  $\text{H}_3\text{Os}_3(\text{CO})_9(\text{SiPh}_3)$  (58%), in addition to unreacted  $\text{H}_2\text{Os}_3(\text{CO})_{10}$  and  $\text{H}_2\text{Os}_3(\text{CO})_{10}(\text{SiPh}_3)_2$ .<sup>11</sup> At high  $\text{HSiPh}_3$  concentrations the reaction proceeds further, forming  $\text{H}_3\text{Os}_3(\text{CO})_9(\text{SiPh}_3)_3$ . We determined the kinetics for disappearance of  $\text{H}_2\text{Os}_3(\text{CO})_{10}$  between 40 and 60 °C under pseudo-first-order conditions. Unfortunately, it did not prove feasible to conduct the kind of study done for  $\text{HSiEt}_3$  because of the smaller equilibrium constant, the lower solubility of  $\text{HSiPh}_3$ , and the number of overlapping IR absorptions due to  $\text{H}_3\text{Os}_3(\text{CO})_{10}(\text{SiPh}_3)$ ,  $\text{H}_3\text{Os}_3(\text{CO})_9(\text{SiPh}_3)$ ,  $\text{H}_2\text{Os}_3(\text{CO})_{10}(\text{SiPh}_3)_2$ , and  $\text{H}_3\text{Os}_3(\text{CO})_9(\text{SiPh}_3)_3$ . At 40 °C the formation of  $\text{H}_3\text{Os}_3(\text{CO})_{10}(\text{SiPh}_3)$  was observable by appearance of the absorption at  $2043 \text{ cm}^{-1}$ , and the plot of absorbance at  $2062 \text{ cm}^{-1}$  vs time showed relaxation toward equilibrium, with the expected decrease in equilibrium concentration of  $\text{H}_2\text{Os}_3(\text{CO})_{10}$  with increasing concentration of  $\text{HSiPh}_3$ ; however, the equilibrium concentration could not be reproducibly established because of the factors above. Measurements at 33–66 mM give estimates of  $K_{\text{eq}}$  of 66(33)  $\text{M}^{-1}$ , but even this estimate is questionable because subsequent reactions cause a systematic error which increases the apparent value of  $K_{\text{eq}}$ . Furthermore,

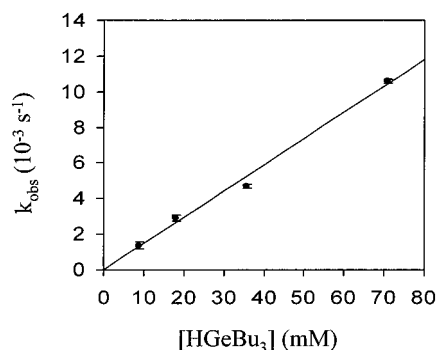


**Figure 4.** Plot of  $k_{\text{obs}}$  vs  $[\text{HGeBu}_3]$  at 30.0 °C.

$k_{\text{obs}}$  (ca.  $1.7 \times 10^{-4} \text{ s}^{-1}$  at  $[\text{HSiPh}_3] = 50 \text{ mM}$ ) did not change within experimental error over the range 33–66 mM; this suggests that  $k_2$  is large relative to  $k_1[\text{HSiPh}_3]$  over this range. In any case, the rate toward equilibrium is slower than it is for  $\text{HSiEt}_3$ , and assuming the same rate law, this must mean that  $k_1$  is less for  $\text{HSiPh}_3$ , since  $k_2$  would be expected to be greater.

**Tributylgermane.** Pomeroy and Ramadan examined the reaction of  $\text{H}_2\text{Os}_3(\text{CO})_{10}$  with  $\text{HGePh}_3$ , but not  $\text{HGeBu}_3$ .<sup>10</sup> The reaction with the latter cleanly produces  $\text{H}_3\text{Os}_3(\text{CO})_{10}(\text{GeBu}_3)$ . The IR spectrum of the solution is very similar (Supporting Information, Figure 2S) to that of the other oxidative addition products. The  $^1\text{H}$  NMR spectrum at  $-70^\circ\text{C}$  is characteristic of a mixture of two of the isomers, one with a cis terminal–bridging hydride pair ( $J_{\text{HH}} = 3 \text{ Hz}$ ; A(1), A(2), or E(3)) and one with a trans terminal–bridging hydride pair ( $J_{\text{HH}} = 12 \text{ Hz}$ ; E(1), E(2), or E(4)), shown in Figure 1. At  $-50^\circ\text{C}$  the coupled hydrides of the major, cis isomer begin to broaden due to exchange; at this temperature the hydrides due to the other isomer remain sharp, as does the singlet hydride resonance for the cis isomer. At room temperature only very broad signals are observed at  $-9.5$  and  $-15.6 \text{ ppm}$ , with sharper, but still broad, peaks at  $-17.0$  and  $-18.4 \text{ ppm}$ . We were unable to isolate pure material because of the high solubility and instability of the product.

Under pseudo-first-order conditions the reaction proceeds to completion. The reaction was conducted in a thermostated cuvette and monitored by UV–visible spectroscopy at 560 nm for  $\text{H}_2\text{Os}_3(\text{CO})_{10}$ . IR spectroscopy was used to verify that the product under pseudo-first-order conditions was the same as that of the stoichiometric reaction. Plots of  $\ln(\text{absorbance})$  vs time are linear, and at 30.0 °C the plot (Figure 4) of  $k_{\text{obs}}$  vs  $[\text{HGeBu}_3]$  is linear with slope  $k_1 = [1.47(0.06)] \times 10^{-1} \text{ M}^{-1} \text{ s}^{-1}$  with an intercept of  $[0.0(0.5)] \times 10^{-3} \text{ s}^{-1}$ . An Eyring plot gives values of  $\Delta H_1^\ddagger = 50(4) \text{ kJ/mol}$  and  $\Delta S_1^\ddagger = -97(13) \text{ J/(K mol)}$ .

**Tributylstannane.** This reaction was examined previously by Ramadan and Pomeroy.<sup>10</sup> The reaction cleanly produces  $\text{H}_3\text{Os}_3(\text{CO})_{10}(\text{SnBu}_3)$ . The IR and NMR spectra are as found by Ramadan and Pomeroy.

Under pseudo-first-order conditions the reaction proceeds to completion. The reaction was monitored using stopped-flow methods and by UV–visible spectroscopy at 560 nm for  $\text{H}_2\text{Os}_3(\text{CO})_{10}$ . IR spectroscopy was used to verify that the product under pseudo-first-order conditions was the same as that of the stoichiometric reaction. Plots of  $\ln(\text{absorbance})$  vs time are linear, and

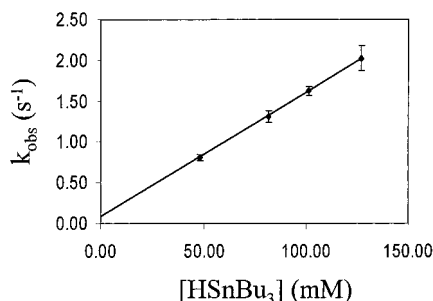


**Figure 5.** Plot of  $k_{\text{obs}}$  vs  $[\text{HSnBu}_3]$  at 25.0 °C.

at 25.0 °C the plot (Figure 5) of  $k_{\text{obs}}$  vs  $[\text{HSnBu}_3]$  is linear with slope  $k_1 = 15.2(0.6) \text{ M}^{-1} \text{ s}^{-1}$  and an intercept of  $0.08(0.06) \text{ s}^{-1}$ , indistinguishable from zero, within experimental error. An Eyring plot gives values of  $\Delta H_1^\ddagger = 44.3(1.9) \text{ kJ/mol}$  and  $\Delta S_1^\ddagger = -73(6) \text{ J/(K mol)}$ . The deuterium kinetic isotope effect, determined from the rate constant for addition of  $\text{DSnBu}_3$ , is  $1.0(0.1)$ .

**Triphenylstannane.** A limited number of experiments were performed with  $\text{HSnPh}_3$ . This reaction was studied previously by Ramadan and Pomeroy.<sup>10</sup> The IR spectrum of the product solution under pseudo-first-order conditions is the same as that reported for  $\text{H}_3\text{Os}_3(\text{CO})_{10}(\text{SnPh}_3)$ . At 25.0 °C the plot of  $k_{\text{obs}}$  vs  $[\text{HSnPh}_3]$  is linear with slope  $k_1 = 0.99(0.12) \text{ M}^{-1} \text{ s}^{-1}$  with an intercept of  $[6(8)] \times 10^{-3} \text{ s}^{-1}$ , indistinguishable from zero within experimental error. An Eyring plot gives values of  $\Delta H_1^\ddagger = 45.6(0.9) \text{ kJ/mol}$  and  $\Delta S_1^\ddagger = -91(3) \text{ J/(K mol)}$ .

## Discussion

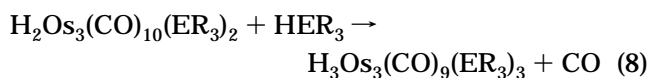
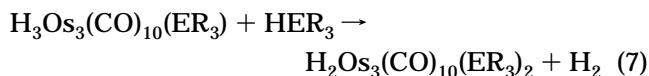
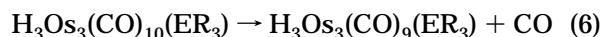
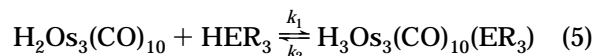
Oxidative additions of group 14 element–hydrogen bonds are fundamental elementary steps in organometallic chemistry and find applications in homogeneous catalysis, especially hydrosilylation.<sup>13</sup> Consequently, there have been many studies of the mechanisms of oxidative additions of C–H and Si–H bonds to metal complexes.<sup>14</sup> The prototypical case is oxidative addition to 16-electron Ir(I) complexes. Hydrides of all members of group 14 are known to add to Ir(I). A comparative study of silane, germane, and stannane ligands has been reported.<sup>15</sup> The mechanism is proposed to be a synchronous, three-center addition, the same as that proposed for oxidative addition of molecular hydrogen. Generally, the facility of oxidative addition increases in the series  $\text{C–H} \ll \text{Si–H} < \text{Ge–H} < \text{Sn–H}$ .

Oxidative addition of  $\text{H–ER}_3$  by saturated triruthenium or triosmium clusters requires prior ligand loss.<sup>16</sup> Several examples of clusters which catalyze hydrosilylation have been reported, including  $[\text{HRu}_3(\text{CO})_{11}]^{1-}$ .<sup>17</sup>

The mechanisms of reductive elimination of C–H bonds from saturated clusters and intramolecular oxidative additions have been examined by several groups.<sup>18</sup> Agostic M–H–C interactions have been reported in a number of hydrocarbyl clusters.<sup>5,18,19</sup> Oxidative addition of the agostic C–H bond of  $\text{HOS}_3(\text{CO})_{10}(\mu\text{-}\eta^2\text{-HCH}_2)$ , yielding  $(\mu\text{-H})_2\text{Os}_3(\text{CO})_{10}(\mu\text{-CH}_2)$ , is very rapid, with a rate constant of  $1 \times 10^{-3} \text{ s}^{-1}$  at 14 °C.<sup>19</sup> The corresponding ethyl to ethylidene conversion has a rate constant of  $1.6 \times 10^{-4} \text{ s}^{-1}$  at  $-10$  °C.<sup>19b</sup> Intermediates containing agostic bonds have been proposed in the reductive elimination of C–H bonds from triruthenium clusters.<sup>18</sup>

Fehlner has proposed that the equilibrium between tautomeric M–H–M and M–H–E sites shifts toward M–H–E as the electronegativity of E decreases.<sup>5</sup>

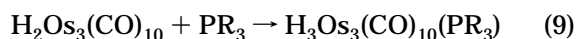
Because unsaturated clusters are very rare, direct examination of the E–H oxidative addition step is generally not feasible. Thus, the observation by Pomeroy and co-workers of the reactions of the unsaturated cluster  $\text{H}_2\text{Os}_3(\text{CO})_{10}$  with  $\text{HER}_3$  (E = Si, Ge, Sn; R = alkyl, Ph) is notable.<sup>10–12,24</sup> As reported by Pomeroy and co-workers, the reactions of  $\text{H}_2\text{Os}_3(\text{CO})_{10}$  with  $\text{HER}_3$  are



The first step, oxidative addition (eq 5), is a reversible reaction for  $\text{HSiR}_3$ , with  $K_{\text{eq}}$  for  $\text{HSiEt}_3$  of  $100 \text{ M}^{-1}$  at 30.4 °C. For the more reactive  $\text{HER}_3$  at room temperature the reaction proceeds to completion, forming  $\text{H}_3\text{Os}_3(\text{CO})_{10}(\text{ER}_3)$  ( $\text{ER}_3 = \text{GeR}_3, \text{SnR}_3, \text{SiHPh}_2$ ). At higher temperatures either CO or  $\text{H}_2$  elimination from the initial product can occur. Thus,  $\text{H}_3\text{Os}_3(\text{CO})_9(\text{SiPh}_3)$  is isolated, rather than  $\text{H}_3\text{Os}_3(\text{CO})_{10}(\text{SiPh}_3)$ , and  $\text{H}_3\text{Os}_3(\text{CO})_{10}(\text{SiEt}_3)$  slowly is converted to  $\text{H}_2\text{Os}_3(\text{CO})_{10}(\text{SiEt}_3)_2$  and then  $\text{H}_3\text{Os}_3(\text{CO})_9(\text{SiEt}_3)_3$ . For the kinetics we only have monitored the initial loss of  $\text{H}_2\text{Os}_3(\text{CO})_{10}$ ; therefore, the kinetic parameters pertain to eq 5.

For each  $\text{HER}_3$  addition studied, the rate law for disappearance of  $\text{H}_2\text{Os}_3(\text{CO})_{10}$  is first-order in  $[\text{H}_2\text{Os}_3(\text{CO})_{10}]$ , as shown by linear plots of  $\ln(k_{\text{obs}})$  vs time, and first-order in  $[\text{HER}_3]$ , as shown by linear plots of  $k_{\text{obs}}$  vs  $[\text{HER}_3]$ , with intercepts of zero, within reasonable experimental errors. The deuterium kinetic isotope effect for  $\text{HSnBu}_3$  is indistinguishable from 1, but the error limits are rather large. Since CO reacts directly with  $\text{H}_2\text{Os}_3(\text{CO})_{10}$  at a faster rate than does  $\text{HSiEt}_3$ , we were unable to test for CO inhibition of the rate. However, the rate constant for  $\text{HSnBu}_3$  addition is unaffected by the saturation of the solution with CO. The large, negative activation entropies are consistent with an associative mechanism.

The initial interaction of  $\text{H–ER}_3$ , acting as a 2e donor via the H–E bond, with  $\text{H}_2\text{Os}_3(\text{CO})_{10}$  is phenomenologically related to additions of Lewis bases such as phosphines; indeed, the mechanistic similarity has been previously noted for additions to Ir(I).<sup>15b</sup> The kinetics for the addition of phosphines to  $\text{H}_2\text{Os}_3(\text{CO})_{10}$  (eq 9) have



been determined.<sup>20</sup> The reaction is associative, with a rate law first order in phosphine concentration. Activation entropies are mostly in the range of  $-90$  to  $-150 \text{ J/(mol K)}$ . The activation volumes (ca.  $-20 \text{ cm}^3 \text{ mol}^{-1}$ ) are also correlated with cone angle of the phosphines. The rate of reaction depends on both the size and the nucleophilicity of the phosphine ligand. The thermodynamically most stable isomer of  $\text{H}(\mu\text{-H})\text{Os}_3(\text{CO})_{10}(\text{PR}_3)$

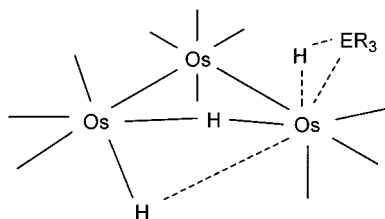


**Figure 6.** Proposed transition state structure for  $\text{HER}_3$  addition, analogous to the one proposed by Poë et al.<sup>20</sup> for  $\text{PR}_3$  addition.

contains an equatorially coordinated  $\text{PR}_3$  ligand and is structurally analogous to isomers A(1) and A(2) in Figure 1.<sup>21</sup> Recently the kinetically favored product of  $\text{PR}_3$  addition has been identified as having an axially coordinated  $\text{PR}_3$ .<sup>22</sup> Kinetics of the  $\text{H}_2\text{Os}_3(\text{CO})_{10}/\text{CO}$  reactions were also investigated.<sup>2a</sup> Both CO dissociation and  $\text{H}_2$  elimination from  $\text{H}(\mu\text{-H})\text{Os}_3(\text{CO})_{11}$  are competitive, with rate constants of  $7 \times 10^{-5}$  and  $4 \times 10^{-6} \text{ s}^{-1}$ , respectively, at 25 °C. Analogous processes are also found for the  $\text{PR}_3$  adducts. Heating  $\text{H}_2\text{Os}_3(\text{CO})_{10}(\text{PR}_3)$  generates  $\text{H}_2\text{Os}_3(\text{CO})_9(\text{PR}_3)$ , while  $\text{H}_2$  loss also occurs.<sup>23</sup> Substituted derivatives preferentially dissociate CO upon heating, with the rate of CO dissociation from  $\text{H}(\mu\text{-H})\text{Os}_3(\text{CO})_{10}(\text{PR}_3)$  decreasing somewhat as the  $\sigma$ -donor ability of  $\text{PR}_3$  increases. Thus, in a number of respects the chemistry of adducts  $\text{H}_2\text{Os}_3(\text{CO})_{10}(\text{PR}_3)$  is very similar to that of  $\text{H}_3\text{Os}_3(\text{CO})_{10}(\text{ER}_3)$ .

All kinetic data obtained for  $\text{HER}_3$  addition to  $\text{H}_2\text{Os}_3(\text{CO})_{10}$  are consistent with the three-center synchronous addition at a single metal center. The rate laws, activation parameters, and relative rates follow the trends established previously for H–E additions to unsaturated monometallic centers. The deuterium isotope effect for  $\text{HSnBu}_3$  addition is closer to 1 than is typically seen for three-center synchronous group 14 element–hydrogen oxidative additions,<sup>13,15a,25</sup> but given the large error limits and the small kinetic isotope effect (kie) for three-center H–E addition (generally in the range 1.2–2), we cannot say that this represents a mechanistic distinction. It should be noted that  $\text{PR}_3$  addition to  $\text{H}_2\text{Os}_3(\text{CO})_{10}$  displays a kie of 1.03–1.28 for deuterium in the hydride sites.<sup>20a</sup> On the basis of the similarity between  $\text{PR}_3$  addition and H– $\text{ER}_3$  addition, the transition state for H–E addition, analogous to that proposed by Poë et al., is shown in Figure 6.

Both the identity of E and R affect the rate constant for H– $\text{ER}_3$  addition. On the basis of the measured activation parameters, at 30 °C the relative rates are  $\text{HSnBu}_3$  (6000) >  $\text{HSnPh}_3$  (400) >  $\text{HGeBu}_3$  (40) >  $\text{HSiEt}_3$  (1). The comparisons of  $\text{HSnBu}_3$  and  $\text{HSnPh}_3$  show a small effect on the rate due to the steric and electronic effects of the substituents on E. However, the reactions are much less sensitive to substituent effects than is shown for group 15 donor ligand addition.<sup>20</sup> This suggests that the primary influence upon the rate constants for  $\text{HER}_3$  addition is due to the properties of the group 14 element–hydrogen bond.

When our data for  $\text{HER}_3$  addition are combined with the results of Poë et al., the selectivity of  $\text{H}_2\text{Os}_3(\text{CO})_{10}$  can be quantified and compared with the selectivities of unsaturated monometal complexes. At 30 °C the

**Table 1. Kinetic Data for Reaction of  $\text{HER}_3$  with  $\text{H}_2\text{Os}_3(\text{CO})_{10}$  in Heptane as in Eq 1**

$\text{HER}_3$	$T$ (°C)	$k_1$ ( $\text{M}^{-1} \text{s}^{-1}$ )	
$\text{HSiEt}_3$	20.0	$[2.02(0.17)] \times 10^{-3}$	$\Delta H_1^\ddagger = 44.9(2.5) \text{ kJ/mol}$
	30.4	$[3.67(0.15)] \times 10^{-3}$	$\Delta S_1^\ddagger = -144(8) \text{ J/(K mol)}$
	40.5	$[7.5(0.7)] \times 10^{-3}$	
	50.0	$[1.27(0.20)] \times 10^{-2}$	
$\text{HGeBu}_3$	20.0	$[6.6(1.0)] \times 10^{-2}$	
	30.0	$[1.47(0.06)] \times 10^{-1}$	$\Delta H_1^\ddagger = 50(4) \text{ kJ/mol}$
	40.0	$[2.47(0.19)] \times 10^{-1}$	$\Delta S_1^\ddagger = -97(13) \text{ J/(K mol)}$
$\text{HSnPh}_3$	25.0	0.99(0.12)	
	45.0	3.71(0.13)	$\Delta H_1^\ddagger = 45.6(0.9) \text{ kJ/mol}$
	60.0	8.4(0.14)	$\Delta S_1^\ddagger = -91(3) \text{ J/(K mol)}$
$\text{HSnBu}_3$	25.0	15.2(0.6)	
	39.5	43.7(2.3)	$\Delta H^\ddagger = 44.3(1.9) \text{ kJ/mol}$
	46.7	53.7(2.8)	$\Delta S_1^\ddagger = -73(6) \text{ J/(K mol)}$
	46.7	48(5) (1 atm CO)	
	53.5	87(7)	

**Table 2. Comparison of  $k$  for  $\text{HER}_3$  Addition to Unsaturated  $\text{Ir}(\text{CO})\text{H}(\text{PPh}_3)_2^{15}$  and  $\text{H}_2\text{Os}_3(\text{CO})_{10}$  Relative to  $\text{PPh}_3$  Addition**

L	$k(\text{PPh}_3)/k(\text{L})$	
	$\text{Ir}(\text{CO})\text{H}(\text{PPh}_3)_2$ , 31 °C in toluene	$\text{H}_2\text{Os}_3(\text{CO})_{10}$ , 30 °C in heptane
$\text{HSiR}_3$	10.6 (R = Ph)	10500 (R = Et)
$\text{HGeR}_3$	0.58 (R = Ph)	270 (R = Bu)
$\text{HSnPh}_3$	0.18	27
$\text{HSnBu}_3$		1.7

second-order rate constants ( $\text{M}^{-1} \text{s}^{-1}$ ) for addition to  $\text{H}_2\text{Os}_3(\text{CO})_{10}$  are as follows:  $\text{PBu}_3$  ( $6.6 \times 10^3$ ) >  $\text{PPh}_3$  (40.0) >  $\text{HSnBu}_3$  (23) >  $\text{HSnPh}_3$  (1.5) >  $\text{HGeBu}_3$  (0.15) > CO ( $6.4 \times 10^{-2}$ ) >  $\text{HSiEt}_3$  ( $3.8 \times 10^{-3}$ ).

The ratio of rate constants for additions of two different reactants to an unsaturated intermediate provides information concerning the selectivity of the intermediate; highly reactive unsaturated metal species typically show competition ratios close to 1, whereas relatively stable unsaturated species display a wide range of competition ratios for different substrates. The competition ratio for the rate constants of  $\text{HER}_3$  addition vs  $\text{PPh}_3$  addition,  $k_{\text{PPh}_3}/k_{\text{E-H}}$ , has been previously determined for  $\text{Ir}(\text{CO})\text{H}(\text{PPh}_3)_2$  (Table 2).<sup>15</sup> The comparison to  $\text{H}_2\text{Os}_3(\text{CO})_{10}$  shows that the unsaturated cluster is more selective not only for oxidative addition of  $\text{HER}_3$  but also for addition of Lewis bases, as evidenced by the larger range of competition ratios vs  $\text{PPh}_3$ .  $\text{H}_2\text{Os}_3(\text{CO})_{10}$  is also more selective than 46-electron intermediates such as  $\text{Os}_3(\text{CO})_{11}$ , where the unsaturation is presumably isolated on a single metal atom.<sup>2b</sup> Poë's transition state adequately accounts for this selectivity, as a significant degree of Os–H–E bond formation and considerable rearrangement of the hydride and carbonyl ligands accompanies addition.

**Acknowledgment.** We acknowledge the essential contribution of R. K. Pomeroy, who provided unpublished results of the characterizations of products and valuable advice concerning these kinetic studies; without his generous contribution, this work would not have been possible. We thank Michael Detty, Associate Professor of Medicinal Chemistry and Chemistry at the University at Buffalo, for use of the stopped-flow equipment. Support for this work was provided in part by grants from the National Science Foundation and from the Mark Diamond Research Fund (to R.J.H.), admin-

(25) (a) Periana, R. A.; Bergman, R. G. *J. Am. Chem. Soc.* **1986**, *108*, 7332. (b) Jones, W. D.; Feher, F. J. *J. Am. Chem. Soc.* **1986**, *108*, 4814.

istered by the Graduate Student Association of the University at Buffalo.

**Supporting Information Available:** Figure 1S, giving (a) IR spectra during the reaction of  $H_2Os_3(CO)_{10}$  with  $HSiEt_3$ , (b) the IR spectrum of  $H_3Os_3(CO)_{10}(SiEt_3)$ , and (c) the IR

spectrum of  $H_3Os_3(CO)_9(SiEt_3)_3$ , and Figure 2S, giving IR spectra of (a)  $H_3Os_3(CO)_{10}(SnBu_3)$  and (b)  $H_3Os_3(CO)_{10}(GeBu_3)$ . This material is available free of charge via the Internet at <http://pubs.acs.org>.

OM000411O